Composite Structures 287 (2022) 115377

Contents lists available at ScienceDirect

Composite Structures

journal homepage: www.elsevier.com/locate/compstruct

Nondestructive examination of polymer composites by analysis of polymer-water interactions and damage-dependent hysteresis

Ogheneovo Idolor, Katherine Berkowitz, Rishabh Debraj Guha, Landon Grace *

North Carolina State University, USA

ARTICLE INFO

Keywords:
Nondestructive examination
Polymer matrix composites
Moisture diffusion
Dielectric properties
Machine learning
Hysteresis

ABSTRACT

Polymer composites are currently replacing metals in applications requiring design flexibility, high strength-to-weight ratio, and corrosion resistance. However, the damage modes in these materials are very different from metals and require specialized techniques to detect internal flaws which may exist even in the absence of visible surface damage. This study proposes a technique for damage detection in polymer composites which uses naturally absorbed moisture as an 'imaging' agent. The locally higher concentration of water in the 'free' state at damaged regions and the tendency of such water to quickly migrate to and from damage sites—exhibiting damage-dependent hysteresis—is leveraged for damage detection. To identify damaged regions, a machine learning approach is adopted using logistic regression to classify local regions as 'undamaged' or 'damaged'. New possibilities resulting from higher sensitivity levels achievable by damage-dependent hysteresis are highlighted, providing a pathway to field deployment of the novel damage detection technique.

1. Introduction

Polymer composites are becoming widely adopted in engineering applications. As they replace metals in various safety–critical moderate temperature service environments [1,2], ascertaining their damage state and fitness for service becomes more crucial. This is confounded by the difference in behavior of these layered materials with regards to damage. Unlike metals, internal damage may be present in the absence of visible surface damage [3,4], especially when paint or coatings are applied. Such damage may be induced during routine operations such as thermal cycling, hail or dropped-tool impact, and cyclic loading. These may lead to matrix cracking, fiber–matrix debonding, and delaminations which may weaken the structure without any warning signs [5,6].

All current nondestructive examination (NDE) techniques for polymer matrix composites have various limitations. These include: inability to characterize beyond a certain depth, limitation to flaws of specific orientation, challenges in flaw localization and characterization, limitations to materials of specific electrical conductivity, and system complexity—requiring a skilled operator [6–8]. Hence, many NDE procedures for safety critical parts have adopted the use of multiple techniques to ascertain structural integrity or they simply incorporate larger design safety factors to compensate for these shortcomings [9]. Therefore novel approaches to NDE of polymer composites are still required to provide reliable, simple, and cost effective solutions. One such approach which may provide a viable solution to many of these challenges is the use of naturally absorbed water as an 'imaging agent' for damage detection in these materials [10–13].

Polymer matrix composites have a tendency to absorb measurable moisture in nearly all operating environments. Studies have shown as much as 2% by weight moisture being absorbed in epoxy based polymer matrix composites [14], and over 0.4% absorbed at steady state for environments with relative humidity as low as 21.5% [15]. This absorption is typically driven by traditional diffusion kinetics [16–22], polymer polarity [23,24], and damage state of the material [25,26]. Studies have shown the effective diffusion process could be deconvoluted into a combination of these multiple independent diffusion processes [26], providing an opportunity to focus on moisture diffusion due to damage state as a means for damage detection [27]. Critical reviews of these studies have been provided in our previous publications [10,27].

Water absorbed by the polymer matrix has been reported to exist in the 'free' state—having no interaction with the polymer matrix, or 'bound' state—interacting with the polymer matrix via secondary bonding interactions such as hydrogen bonding with polar functional groups, dipole–dipole attractions, or van der Waals forces with polymer chains [25,28–30]. These interactions restrict the mobility of the water

* Corresponding author at: Department of Mechanical and Aerospace Engineering, North Carolina State University, 911 Oval Drive, Raleigh, NC 27695, USA.
E-mail address: landon_grace@ncsu.edu (L. Grace).

https://doi.org/10.1016/j.compstruct.2022.115377
Received 6 July 2021; Received in revised form 4 January 2022; Accepted 10 February 2022
Available online 15 February 2022

molecules, limiting their ability to rotate with an electromagnetic field at microwave frequencies and also influencing the resonant frequency of the oxygen-hydrogen bond vibrations [11,31,32]. These effects have enabled the ability to characterize these polymer-water interactions using near-infrared spectroscopy [12,32] and microwave-frequency dielectric properties [11,33,34], amongst other techniques [28,35,36].

Damage which creates voids within the polymer matrix in the form of matrix cracks, fiber–matrix debonding, and delamination create ideal sites for water to exist in the free state [28,37,38]. While, in undamaged regions water molecules behave differently due to their close proximity to the polymer network, leading to interactions that limit it to the bound state [28,37,39]. Hence, a higher concentration of free water could be an indication of damage. Furthermore, leveraging such a molecular level phenomenon for NDE could enable damage detection at sub-micron-scale levels—a limitation of current techniques [10].

In our previous work, we demonstrated how polymer-water interactions can be characterized and the effects of localized impact damage on the water state distribution [10]. We further investigated humidity fluctuations in the ambient environment leading to loss or gain of total moisture and its effect on the water state distributions in a damaged polymer composite laminate [27]. We concluded that such variations in moisture content had a significant effect on the sensitivity to damage of polymer-water interactions. Single-mode sorption was also observed in undamaged regions and dual-mode sorption in damaged regions. This led to the discovery of damage-dependent hysteresis in polymer composites, providing a reliable basis for nondestructive damage detection [27]. However, in these studies, only a qualitative determination of damage state based on polymer-water interactions and damage-dependent hysteresis was outlined. Hence, an approach to map the location of damaged areas in polymer composites is required.

This study builds on knowledge gained in behavior of polymer-water interactions and explores ways to quantitatively define the extent of localized damage in a polymer matrix composite. Polymer-water interactions are characterized using microwave-frequency dielectric properties by coupling a split post dielectric resonator to a vector network analyzer [40]. Similar to scans in our previous work [27], water state distributions are obtained by 2-dimensional scans showing spatial variation in relative permittivity (real part of dielectric constant) across the polymer matrix composite laminate. The first method explored is based on a single scan taken during the absorption process, while the second method is based on multiple scans taken during the absorption and desorption processes—an approach based on damage-dependent hysteresis. To map out the damaged regions and demonstrate predictability, a machine learning based approach is adopted. Finally, progress towards a highly sensitive generalized approach is discussed, and further considerations required to achieve this are presented.

2. Materials and methods

2.1. Experimental details

A detailed description of the experimental procedure used in this study has been provided in our previous work [27]. These include a description of materials used, fabrication processes, material properties, sample conditioning, impact setup, dielectric measurement, and the data collection process at each measurement interval. Reference should be made to Section 2 (Experimental) of the publication for these details [27]. Also, a discussion on how confounding factors were mitigated has been provided in Section 3.1 of our previous study [27]. Hence, the rest of this section will focus on details relevant to data processing that would enable successful damage prediction.

2.2. Machine learning model

In order to determine the damage state across the laminate, a prediction of 'undamaged' or 'damaged' would be required at all points. This can be interpreted as a binary classification problem which can be solved using various machine learning models, i.e. neural network, logistic regression, clustering, etc. Due to the fairly low number of predictive features, a logistic regression model is employed. The machine learning model is implemented using MATLAB® and optimization is achieved using the 'fminunc' (function minimization unconstrained) advanced optimization function. The fminunc function requires a cost function as the main input. The cost function outputs the prediction error for a set of model parameters (weights) and their gradients. Other inputs required include optimization options such as maximum number of iterations and 'GradObj' which is set to 'on'—specifying that the gradient would be provided at each iteration. Initial parameter values are also required.

The logistic regression cost function is composed of two parts—a log-loss cost term and a regularization term (see Equation (1)) [41,42]. The log-loss cost term is ideal to avoid local minimums during optimization of the logistic regression model. The regularization term is included to avoid over-fitting the data by adjusting the regularization parameter λ. This parameter determines how much effect the term has on the cost function [41]. The gradient function is the partial derivative of the cost function with respect to the parameters (see Equation 2) [41]. This helps point the algorithm in the direction of minimum cost for subsequent iterations. Note that the derivative of the cost function with respect to the first parameter (θ_j) is not regularized (hence Equation (2a)) [41].

$$\textbf{Cost}: J(\theta) = \frac{1}{m}\sum_{i=1}^{m}\left[-y^{(i)}\log\left(h_\theta\left(x^{(i)}\right)\right) - \left(1-y^{(i)}\right)\log\left(1-h_\theta\left(x^{(i)}\right)\right)\right] + \frac{\lambda}{2m}\sum_{j=1}^{n}\theta_j^2 \tag{1}$$

$$\textbf{Gradient}: \frac{\partial J(\theta)}{\partial \theta_j} = \frac{1}{m}\sum_{i=1}^{m}\left(h_\theta\left(x^{(i)}\right) - y^{(i)}\right)x_j^{(i)} \quad \text{for } j = 0 \tag{2a}$$

$$\frac{\partial J(\theta)}{\partial \theta_j} = \left(\frac{1}{m}\sum_{i=1}^{m}\left(h_\theta\left(x^{(i)}\right) - y^{(i)}\right)x_j^{(i)}\right) + \frac{\lambda}{m}\theta_j \quad \text{for } j \geq 1 \tag{2b}$$

where

i is the example number
j is the parameter number
m is total number of examples
n is the total number of parameters
θ_j is the weight for the j^{th} feature
$x^{(i)}$ is the input feature of the i^{th} example
$y^{(i)}$ is the output for the i^{th} example
h_θ is the predicted output for an example based on a set of θ parameters.
λ is the regularization parameter

3. Results and discussion

3.1. Effect of moisture on damage sensitivity

Gravimetric moisture uptake and moisture loss behavior with time has been provided in our previous study showing how absorption/desorption history affect the sensitivity to damage of polymer-water interactions [27]. Fig. 1 shows the effect of moisture content on polymer-water interactions by observing the spatial variation in relative permittivity with increasing moisture content for a 2 and 3-Joule impact-damaged specimen. An increased sensitivity to damage is observed with increasing moisture content. Also, with increasing moisture content a subtle increase in relative permittivity is observed in the undamaged regions. This is indicative of a higher proportion of free water relative to bound water migrating to the damaged region, while

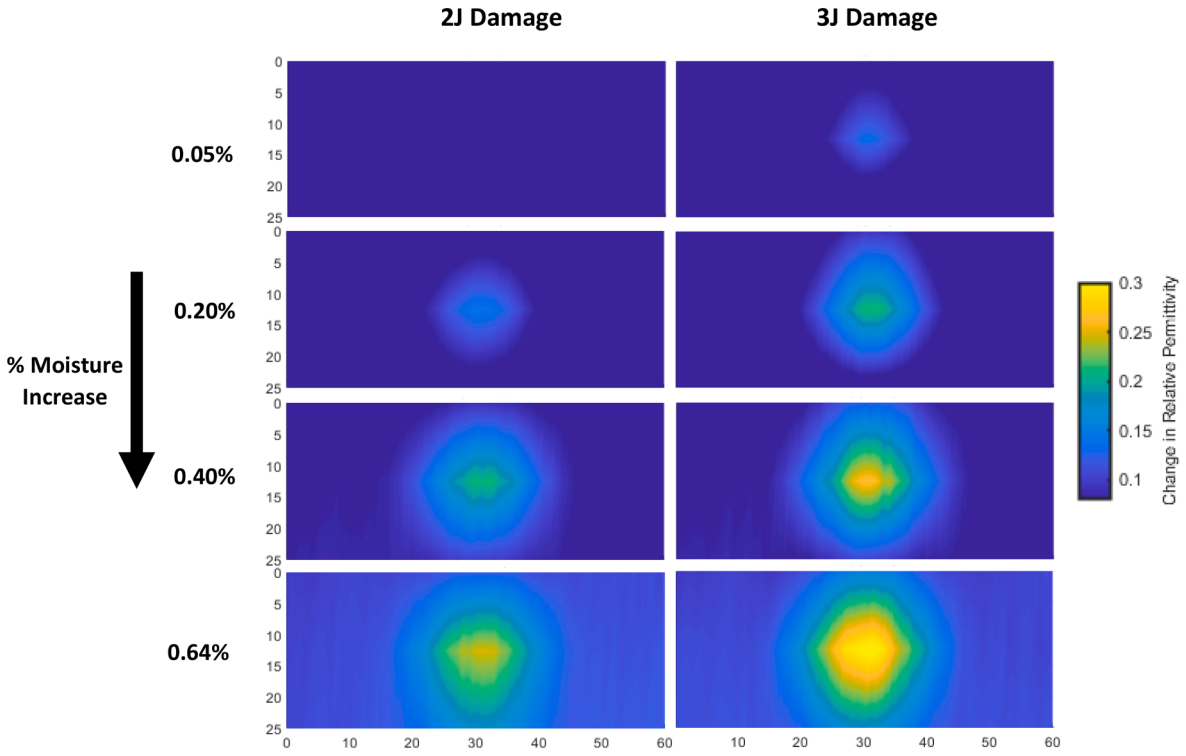

Fig. 1. Effect of moisture content on sensitivity of polymer-water interactions to damage. Length measurements in mm.

the gradual increase in relative permittivity in the undamaged region is primarily driven by a higher proportion of physically or chemically bound water [10]. This therefore establishes that the sensitivity to damage is not only a function of the extent of physical damage but also the moisture content, forming a sensitivity triangle comprising moisture content, extent of damage, and relative permittivity as the three main influences. Thus, the relative permittivity and moisture content could serve as ideal predictors of the damage state of a moisture contaminated polymer composite laminate.

3.2. Input features for machine learning model

Based on conclusions from Section 3.1 above, the total moisture content along with the relative permittivity at the various points across the laminate would be ideal input features in a machine learning model for determining the damage state at each point across a laminate. These are designated as features x_1 and x_2 respectively, while $\boldsymbol{x}$ is the feature vector. The first step is to label the example data which would serve as input for training the logistic regression model. To achieve this, a representative scan image with pixel sizes of 0.5 mm is superimposed on

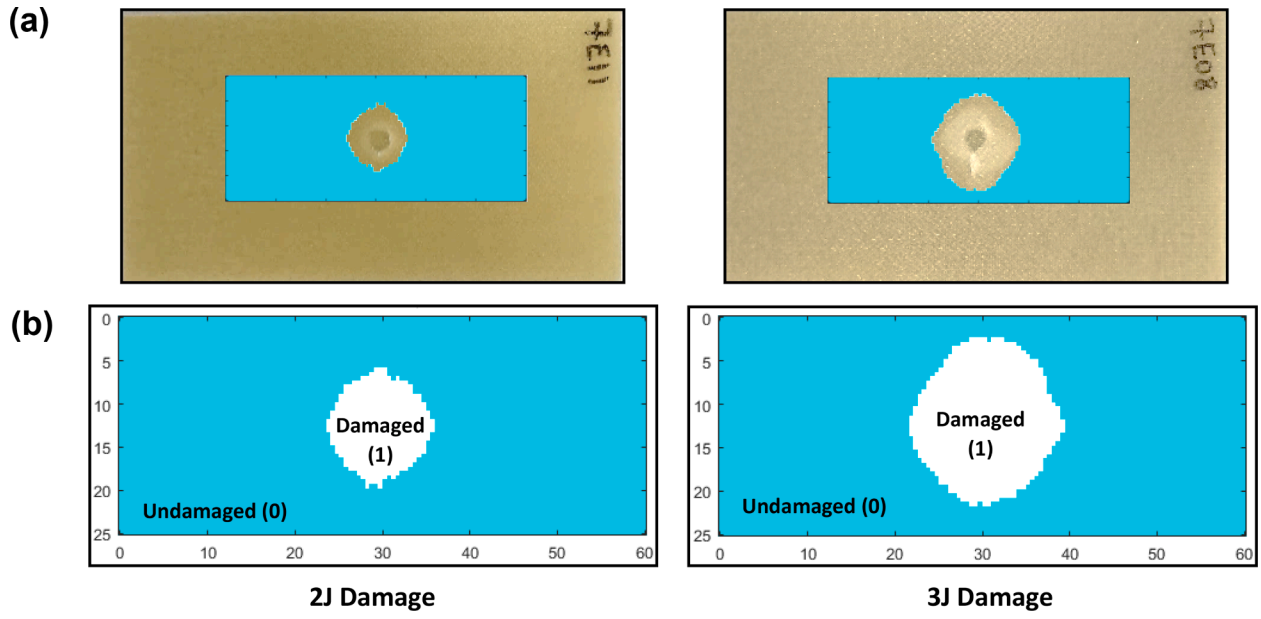

Fig. 2. (a) Representative scans superimposed on test specimens to mark damaged regions (b) Labelled representative scans used as training examples. Length measurements in mm.

an actual specimen. The relative permittivity at the edge of the damaged region is then determined as the threshold relative permittivity, above which any point would be labelled as damaged (see Fig. 2 (a)). Since the output label ($\boldsymbol{y}$) can only be undamaged or damaged, this can be modelled as a binary classification problem [41], where the undamaged regions have an output label of '0' and the damaged regions '1'. Therefore, the final labelled examples would be as shown in Fig. 2 (b).

To achieve a non-linear decision boundary with just two features, a combination of various powers of x_1 and x_2 up to the 6th power is used to generate the feature vector ($\boldsymbol{x}$) [43]. This results in a feature vector comprising 28 elements (see Equation (3)). Since the desired output is either a '0' or '1', a sigmoid function is employed according to Equation (4) to limit the predictions from this vector to between 0 and 1 [41].

$$\textbf{Feature vector}: \boldsymbol{x} = \begin{bmatrix} 1 & x_1 & x_2 & x_1^2 & x_1x_2 & x_2^2 & x_1^3 \ldots x_1x_2^5 & x_2^6 \end{bmatrix} \tag{3}$$

$$\textbf{Sigmoid Function}: h_\theta(\boldsymbol{x}) = \frac{1}{1 + e^{-\boldsymbol{\theta}^T \boldsymbol{x}}} \tag{4}$$

3.3. Training the machine learning model

The total sample consists of four 2-Joule and 3-Joule impact damaged specimens (total of eight specimens). The training data set comprises 75% of the total sample size (three 2-Joule and 3-Joule impacted specimens—total of six), while 25% (a 2-Joule and 3-Joule specimen—total of two) is reserved for the test data set. To eliminate any bias in test set selection, all 16 possible groupings of the specimens into training and test sets were evaluated. Results in Table 1 shows variation in training set accuracy of only 0.15% between upper and lower 95% confidence bounds for the 16 possible combinations, indicating a high level of predictability regardless of grouping. Fig. 3(a) shows a distribution of undamaged and damaged data points as a function of relative permittivity and moisture content for a typical grouping. An interface between the undamaged and damaged data points can be observed. The goal of the model training process is to identify the ideal interface, or decision boundary, between the undamaged and damaged regions. To determine this ideal decision boundary, the model weights ($\boldsymbol{\theta}$) for the input parameters at the minimum cost is required. Equations 1 and 2 provides the cost and gradient functions to be computed at each iteration, where a unique set of $\boldsymbol{\theta}$ is tested. The effect of the regularization parameter remained negligible even when reduced to the adopted value of 0.0001, indicating minimal effect of the regularization term in preventing over-fitting. This is simply due to the large number of data points (~550,000) used in training the model. Therefore, an additional cross-validation set to optimize this parameter is not required. After training the model, the optimum decision boundary is obtained as shown in Fig. 3(a); this is used in developing the prediction model in Fig. 3(b). The boundary appears to be fairly linear; therefore, a linear model would be a reasonable approximation for prediction of damage based on only moisture content and relative permittivity.

3.4. Damage predictions

Using the prediction model developed in Fig. 3(b), each pixel in the 2-dimensional relative permittivity scan is evaluated and—depending on where it falls on the prediction model—is classified as an undamaged or a damaged point. Fig. 4 shows predictions on a typical test set for a 2-Joule and 3-Joule impact-damaged specimen at various moisture contents. When compared to scans in Fig. 1 where the relative permittivity increased with moisture content, the prediction model compensates for this and effectively predicts the damaged regions at different moisture content. Table 1 shows the associated accuracies in predicting these damaged areas, being at least 95% accurate. Fig. 4 also shows a severe under-prediction for the 2-Joule specimen at and below 0.1% moisture by weight. This indicates that detecting lower levels of damage require higher amounts of moisture to increase sensitivity of the technique. Therefore, a minimum level of moisture content could be established based on the desired level of damage to be detected. Note that studies have reported over 2% moisture absorbed in polymer matrix composites [14], and an average steady state moisture content of 0.44% at humidity levels as low as 21.5% [15]. Such levels of moisture provide adequate sensitivity even for impact damage as low as 2-Joule.

Table 1
Training and Test Set Accuracy.

	95% Confidence Interval (%)	
	Upper Bound	Lower Bound
Training Set Accuracy	97.35	97.20
Test Set Accuracy – 2-Joule Impact	98.22	96.88
Test Set Accuracy – 3-Joule Impact	96.78	95.36

3.5. Limitations of damage detection based on absorption process scans

The damage detection approach described so far is based on absorption process scans and relative differences in relative permittivity. It has the advantage of requiring only one scan and being simple to implement by training a machine learning model. However, it also has some limitations which could hamper deployment as a damage detection technique for polymer composites. Firstly, the need to subtract the relative permittivity response of the initial dry-pristine condition from subsequent moisture contamination states is not very practical for many field applications, where no prior knowledge exists of the dielectric response of the composite part [6]. Secondly, there is some uncertainty due to possible desorption before or during scanning, which could lead to decreased sensitivity to damage [27]. Thirdly, in the presence of signal noise due to confounding factors [27], relatively low damaged-to-undamaged ratios as shown in Fig. 5 may result in difficulty in detecting relative permittivity change as a result of damage. Here we define the damaged-to-undamaged ratio as the largest change in relative permittivity at the damaged region divided by the average relative permittivity change of the undamaged regions. This provides an idea of how sensitive the technique is to damage. Finally, the prediction model developed would be specific to only a unique combination of materials and moisture absorption process. Hence, different models would be required for other material systems or test specimens which undergo a different moisture absorption process or produce a different dielectric response.

3.6. Damage-dependent hysteresis

The adoption of a damage detection technique based on the damage-dependent hysteresis behavior in polymer composites could provide a viable solution to many of the challenges identified in Section 3.5 using absorption process scans. The possibility of leveraging the hysteresis effect as a reliable basis for damage detection was proposed in our previous work [27], where we showed how it can be used to eliminate the uncertainty resulting from fluctuations in total moisture content. We also showed that the size of the hysteresis loops can be correlated to the extent of physical damage within the polymer composite (see Fig. 6). Therefore, a way to quantify the size of the hysteresis loop to determine the damage state is required. One way to achieve this is to fit a linear trend line to the absorption–desorption data and calculate the residual sum of squares (RSS). For an undamaged region, the linear trend would fit closely, generating a relatively low RSS. While for a damaged region, a poor linear fit would be achieved leading to a significantly higher RSS (see Fig. 7 (a) and (b)).

The use of damage-dependent hysteresis also presents an opportunity to eliminate the need for subtraction of the dry-pristine relative permittivity baseline, which may be impractical in many scenarios. By excluding the starting data point at the origin and introducing an intercept term for the linear fit, the use of absolute values of relative

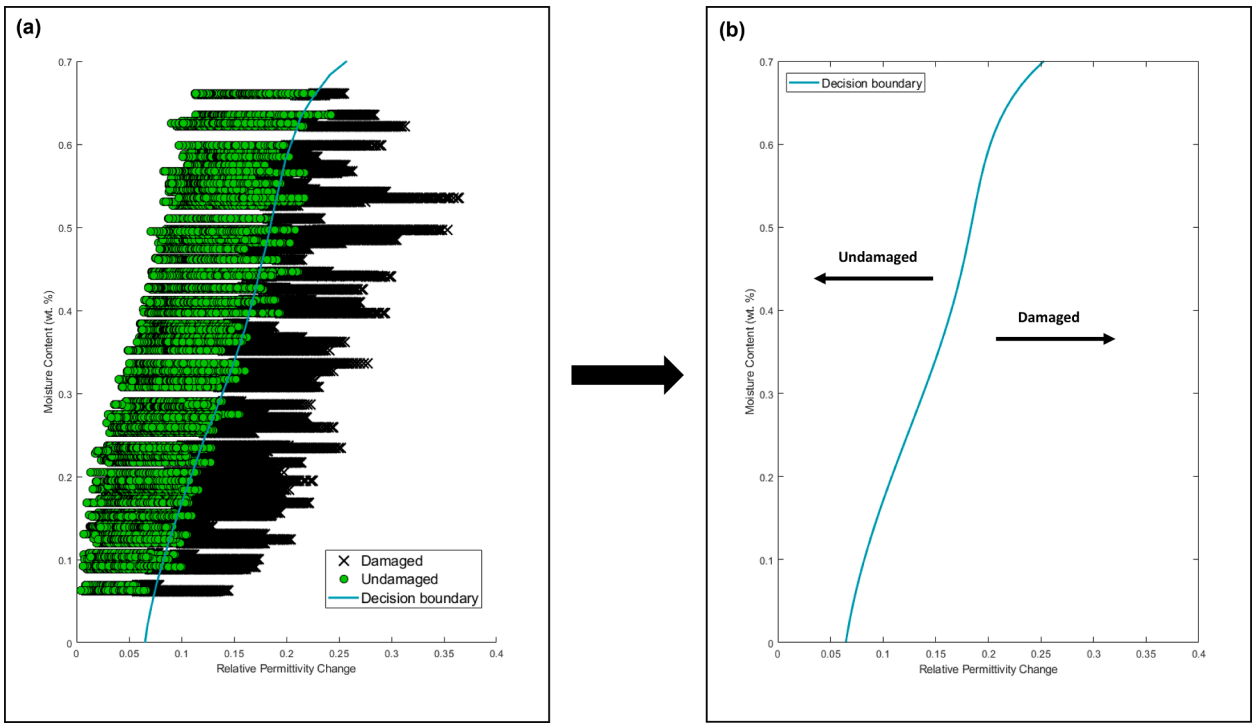

Fig. 3. (a) Plot of example data showing undamaged and damaged data points. (b) Final prediction model.

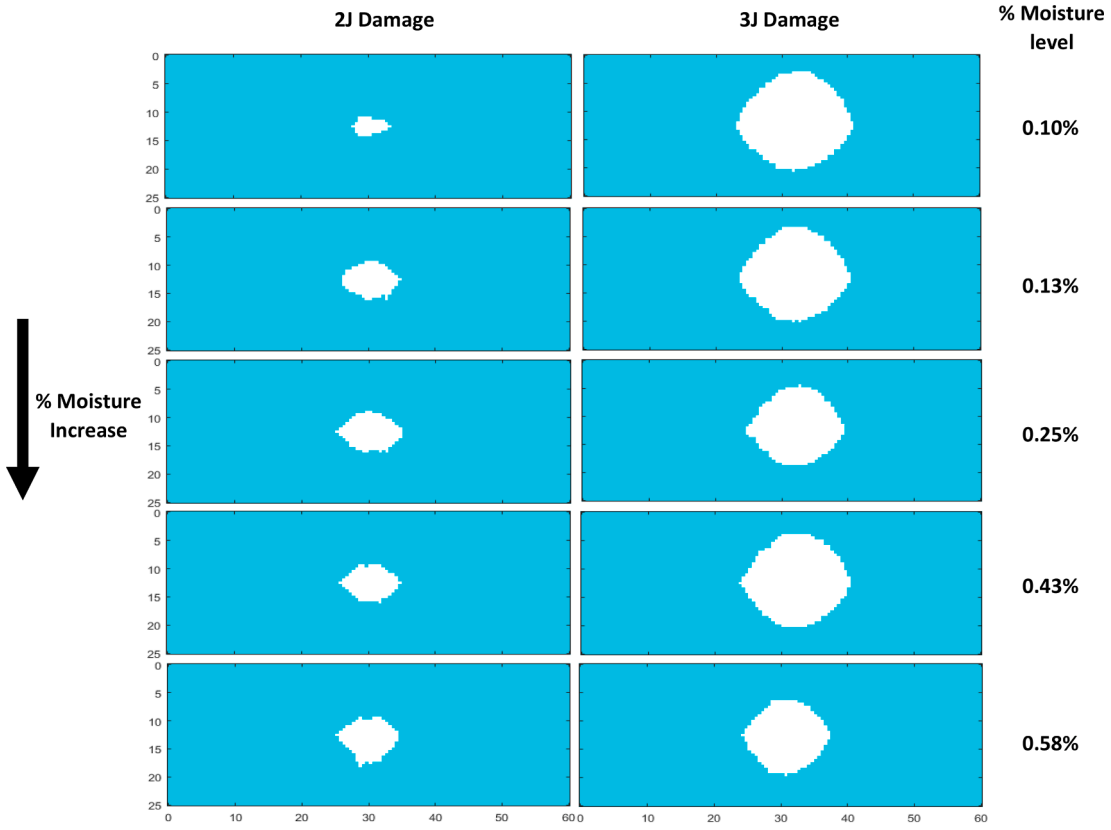

Fig. 4. Damage predictions on test set. Length measurements in mm.

permittivity becomes possible. Fig. 7(c) and (d) shows the plots achieved by incorporating these changes. The undamaged region plot in Fig. 7(c) remains almost identical to Fig. 7(a) due to their close linear fit. While for the damaged region absorption–desorption plot in Fig. 7(d), more flexibility is provided to the linear fit with the introduction of an intercept term—enabling a better fit relative to that in Fig. 7(b). Since our damage quantification metric is based on RSS, a better linear fit would lead to a lower RSS and hence less sensitivity to damage.

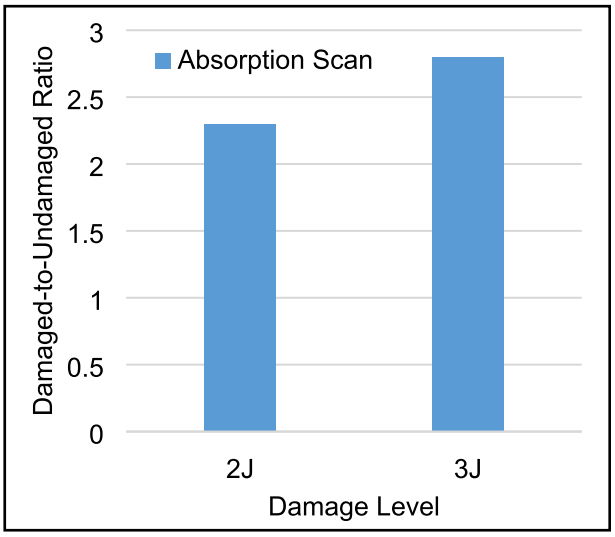

Fig. 5. Damaged-to-undamaged ratio for 2 and 3-Joule impact damaged specimens at 0.6% moisture by weight.

A 2-dimensional plot showing variation in RSS can be produced by generating an absorption–desorption plot for each point on the laminate and then fitting a linear trend line to the plot (see Fig. 8). The result obtained is similar to the change in relative permittivity variation scans in Fig. 1, with the RSS scans also showing significantly higher RSS at the damaged regions. However, the RSS scan has some key advantages. Unlike the absorption process scans where the relative permittivity of the undamaged region also increases gradually with moisture content (see Fig. 1), for damage-dependent hysteresis the undamaged regions remains essentially flat and close to zero for any scenario. This can be clearly seen in Fig. 9, which shows the variation in RSS for the middle axis (a horizontal line through the middle) of scans in Fig. 8. Also, the sensitivity to the extent of damage is much more pronounced as seen in Figs. 8 and 9, showing much better distinction between damage levels. The magnitude of this difference is appreciated when we compare the undamaged-to-damaged ratio for damage-dependent hysteresis and absorption process scans as shown in Figs. 5 and 10. Damage-dependent hysteresis shows undamaged-to-damaged ratios close to 400 for the 3-Joule damaged specimens, compared to just 2.8 for the absorption process scan. This is over two orders of magnitude greater, which suggests sensitivity improvements of similar magnitude. Consequently, training a machine learning model based on damage-dependent hysteresis data should produce more accurate predictions with fewer limitations.

Also, the loss in sensitivity in moving to a generalized process, described earlier, can be observed in Fig. 10. This loss appears to be tolerable considering the very high sensitivity levels being achieved with damage-dependent hysteresis.

3.7. New possibilities with damage-dependent hysteresis

With significantly higher levels of sensitivity now achievable with damage-dependent hysteresis, new possibilities in the development of a nondestructive examination technique based on polymer-water interactions may become feasible; thus providing additional flexibility in factors that influence sensitivity to damage such as moisture variation range, detectable level of damage, number of scans required, sensitivity of dielectric characterization technique, and effects of confounding factors.

A smaller moisture variation range may now be adequate to observe the hysteresis effect. The method could simply take advantage of the rapid non-linear increase during absorption and similar decrease during desorption [10,27], rather than waiting for much slower moisture uptake in the undamaged region. This could lead to a faster damage detection process. Alternatively, the higher sensitivity would allow for detection of lower damage levels, which could enable sub-micron scale damage detection in polymer composites. Such resolution is necessary for detecting damage at the initiation phase [44], which could enable better prediction of yield point and remaining useful life in polymer composites.

The number of scans required to generate adequate number of data points for the hysteresis loop could also be reduced since the sensitivity is also closely related to the number of points used in calculating the RSS. Increasing the number of data points would add smaller RSS values to undamaged regions but much larger values to damaged regions, leading to increased sensitivity. Hence depending on the level of sensitivity required, the number of required scans could be optimized. Interpolations between scans to generate additional data points could be another potential means for increasing sensitivity.

Another factor which affects sensitivity is the dielectric characterization method. The use of more robust but less sensitive dielectric characterization techniques could now be possible with the higher sensitivity. The split post dielectric resonance technique which was used

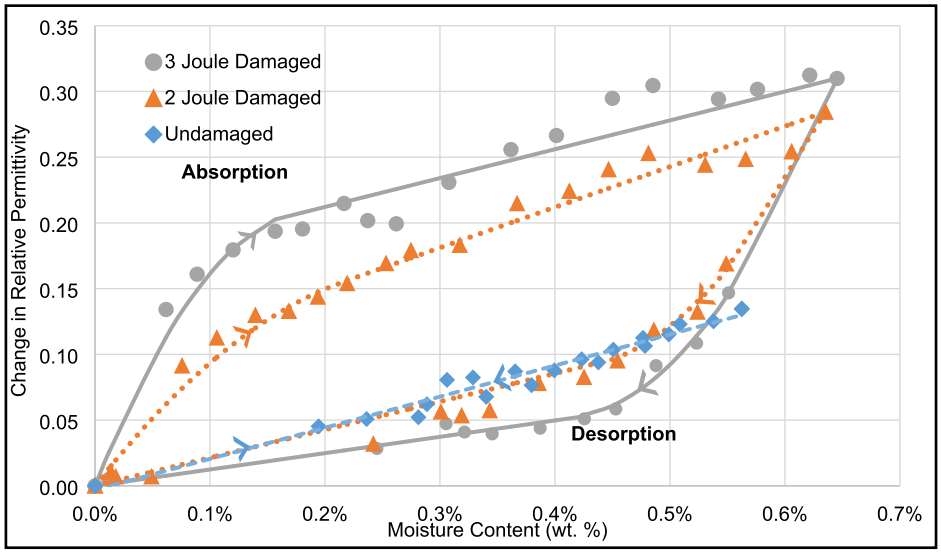

Fig. 6. Plot showing damage-dependent hysteresis in relative permittivity [27].

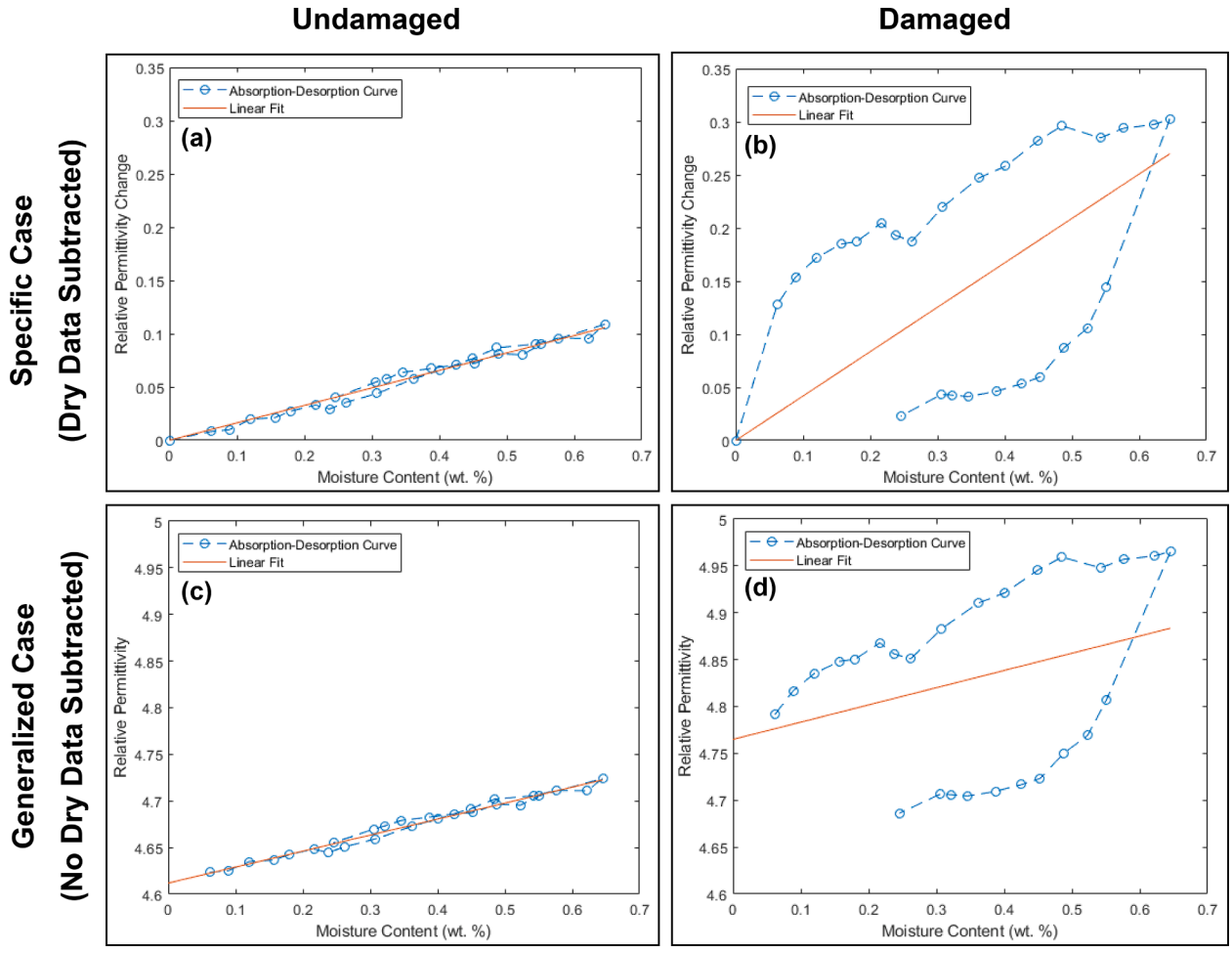

Fig. 7. Linear fit to absorption–desorption data for a 3-Joule impact damage specimen in (a) an undamaged region for specific case (b) a damaged region for specific case (c) an undamaged region for generalized case (d) a damaged region for generalized case.

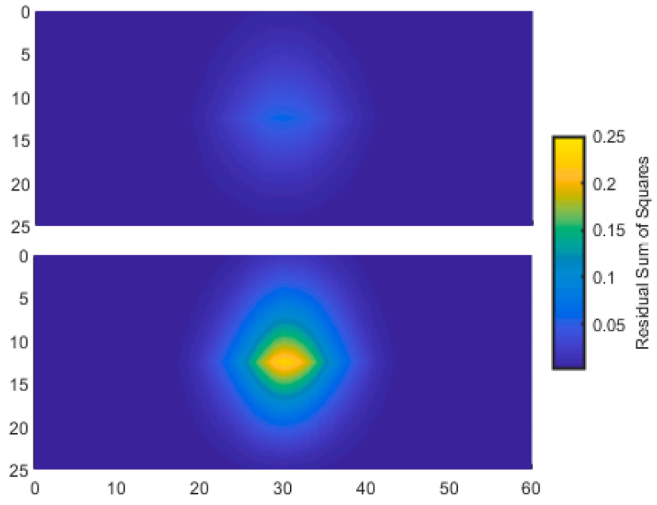

Fig. 8. 2-diemsional spatial variation in residual sum of squares for a 2-Joule and 3-Joule impact damaged laminate. Length measurements in mm.

for dielectric property characterization is currently the most accurate technique, with only 0.3% uncertainty [45,46]. However, it has very limited specimen size requirements—0.95 mm, 1.95 mm, and 3.1 mm maximum thickness for 10 GHz, 5 GHz, and 2.4 GHz. Also they work in transmission mode [10,27], requiring access to both sides of a laminate. The less restrictive free space technique could be used in reflectance mode, allowing one-sided characterization in applications where only one side of the laminate is accessible. The downside of the free space technique is its reduced accuracy [46], which could be compensated for by the higher sensitivity of the damage-dependent hysteresis technique.

Further studies are required to confirm how each of these newly unlocked possibilities can be leveraged in developing this method from the current laboratory scale to suitability for field applications. Field deployment studies could begin with marine applications, which may be a natural fit for the damage-dependent hysteresis technique. During service, the extreme exposure to moisture can accelerate the absorption phase, while desorption can be achieved naturally during dry docking for maintenance. Also, since polymers of various material chemistries are being used as matrix material and majority of polymer composites in service are painted and coated, it would be useful to know how these affect moisture uptake, microwave signal degradation, distribution of the various water states in a damaged polymer composite, and ultimately the ability to detect damage using this technique.

4. Conclusion

This study provides an avenue for the nondestructive detection of damage in polymer matrix composites by analysis of polymer-water interactions and damage-dependent hysteresis. We build on our prior studies which investigated the effect of damage on water state distribution and the role fluctuations in total moisture content plays in determining their degree of sensitivity to damage. These studies

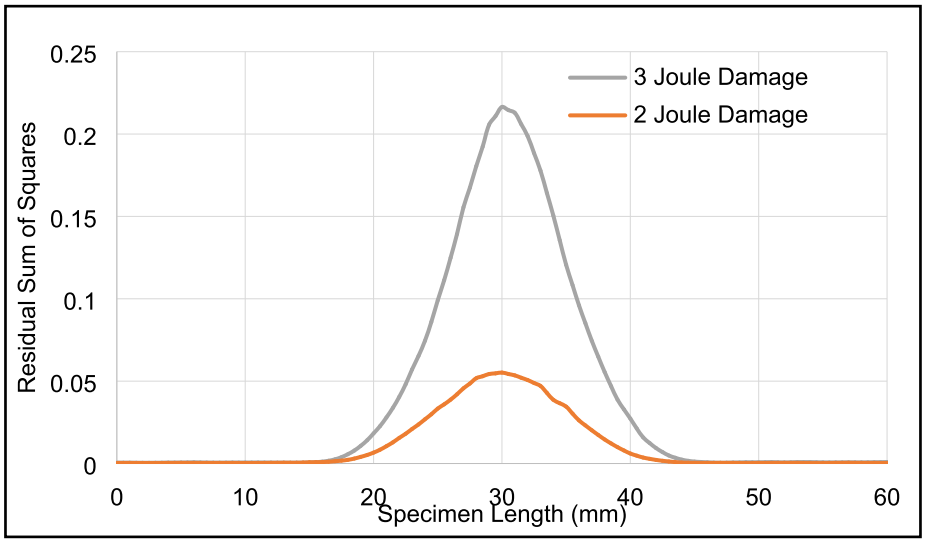

Fig. 9. Residual sum of squares variation along the middle axis of a 2-Joule and 3-Joule impact damaged laminate.

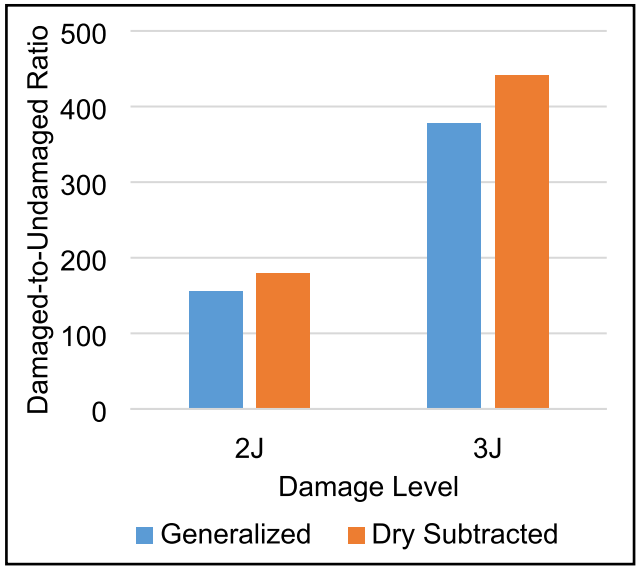

Fig. 10. Damaged-to-undamaged ratio for 2 and 3-Joule impact damaged specimens using damage-dependent hysteresis.

concluded that a higher proportion of free water exists in voids created due to damage in a moisture-contaminated polymer composite, and that damage-dependent hysteresis exists for absorption and desorption processes. In this study, a machine learning approach for quantifying damaged regions in a polymer composite is presented. A logistic regression model is trained and evaluated, showing satisfactory performance in mapping out damaged regions in a polymer matrix composite laminate. Furthermore, a generalized basis for nondestructive examination of polymer composites based on damage-dependent hysteresis is demonstrated. This is shown to achieve sensitivity levels which are over two orders of magnitude greater than results obtained by leveraging polymer-water interactions through a single absorption process scan. This improvement in sensitivity enables new possibilities which would allow further development of the technology and scale-up from the lab to a system ready to be applied in the field.

CRediT authorship contribution statement

Ogheneovo Idolor: Conceptualization, Methodology, Investigation, Software, Data curation, Visualization, Formal analysis, Writing – original draft. **Katherine Berkowitz:** Writing – review & editing, Investigation. **Rishabh Debraj Guha:** Writing – review & editing. **Landon Grace:** Conceptualization, Supervision, Project administration, Funding acquisition, Resources, Writing – review & editing.

Declaration of Competing Interest

The authors declare that they have no known competing financial interests or personal relationships that could have appeared to influence the work reported in this paper.

Acknowledgments

This work was supported by the National Science Foundation [Grant No. CMMI-175482]. The assistance of Bassey Enebong Bassey is appreciated for aiding with graphical visualizations during the project.

Data availability

The raw/processed data required to reproduce these findings cannot be shared at this time as the data also forms part of an ongoing study.

References

[1] Boyle MA, Martin CJ, Neuner JD, Corporation H. Epoxy resins. Composites, vol. 21, ASM International; 2001, p. 90–6. https://doi.org/10.31399/asm.hb.v21.a0003363.
[2] Stenzenberger H, Gmbh T. Bismaleimide Resins. Composites, vol. 21, ASM International; 2001, p. 97–104. https://doi.org/10.31399/asm.hb.v21.a0003364.
[3] Meola C, Carlomagno GM. Non-destructive evaluation (NDE) of aerospace composites: Detecting impact damage. 2013. https://doi.org/10.1533/9780857093554.3.367.
[4] Bossi RH, Giurgiutiu V. Nondestructive testing of damage in aerospace composites. Polym Compos Aerosp Ind 2014:413–48. https://doi.org/10.1016/B978-0-85709-523-7.00015-3.
[5] Riccio A, De Luca A, Di Felice G, Caputo F. Modelling the simulation of impact induced damage onset and evolution in composites. Compos Part B Eng 2014;66:340–7. https://doi.org/10.1016/j.compositesb.2014.05.024.
[6] Nsengiyumva W, Zhong S, Lin J, Zhang Q, Zhong J, Huang Y. Advances, limitations and prospects of nondestructive testing and evaluation of thick composites and sandwich structures: A state-of-the-art review. Compos Struct 2021;256:112951. https://doi.org/10.1016/j.compstruct.2020.112951.

[7] Gholizadeh S. A review of non-destructive testing methods of composite materials. Procedia Struct Integr 2016;1:50–7. https://doi.org/10.1016/j.prostr.2016.02.008.

[8] Jolly MR, Prabhakar A, Sturzu B, Hollstein K, Singh R, Thomas S, et al. Review of non-destructive testing (NDT) techniques and their applicability to thick walled composites. Procedia CIRP 2015;38:129–36. https://doi.org/10.1016/j.procir.2015.07.043.

[9] Zhu T-L. A reliability-based safety factor for aircraft composite structures. Comput Struct 1993;48(4):745–8. https://doi.org/10.1016/0045-7949(93)90269-J.

[10] Idolor O, Guha RD, Berkowitz K, Geiger C, Davenport M, Grace L. Polymer-water interactions and damage detection in polymer matrix composites. Compos Part B Eng 2021;211:108637. https://doi.org/10.1016/j.compositesb:2021.108637.

[11] Idolor O, Guha R, Grace L. A dielectric resonant cavity method for monitoring of damage progression in moisture-contaminated composites. Am. Soc. Compos. 2018, vol. 2, Lancaster, PA: DEStech Publications, Inc.; 2018. https://doi.org/10.12783/asc33/25963.

[12] Idolor O, Guha R, Berkowitz K, Grace L. Damage detection in polymer matrix composites by analysis of polymer-water interactions using near-infrared spectroscopy. Am. Soc. Compos. 2020, Lancaster, PA: DEStech Publications, Inc.; 2020. https://doi.org/10.12783/asc35/34874.

[13] Idolor O, Guha R, Bilich L, Grace L. 2-dimensional mapping of damage in moisture contaminated polymer composites using dielectric properties. Am. Soc. Compos. 2019, Lancaster, PA: DEStech Publications, Inc.; 2019. https://doi.org/10.12783/asc34/31312.

[14] Zafar A, Bertocco F, Schjødt-Thomsen J, Rauhe JC. Investigation of the long term effects of moisture on carbon fibre and epoxy matrix composites. Compos Sci Technol 2012;72(6):656–66. https://doi.org/10.1016/j.compscitech.2012.01.010.

[15] Springer GS. Moisture content of composite under transient conditions. J Compos Mater 1977;11:107–22.

[16] Fan Y, Gomez A, Ferraro S, Pinto B, Muliana A, Saponara VL. Diffusion of water in glass fiber reinforced polymer composites at different temperatures. J Compos Mater 2019;53(8):1097–110. https://doi.org/10.1177/0021998318796155.

[17] Rodriguez LA, Damley-Strnad A, Grace LR. Temperature and anisotropy effects in the application of the hindered diffusion model to composite laminates. J Reinf Plast Compos 2019;38(13):628–39. https://doi.org/10.1177/0731684419839220.

[18] Rodriguez LA, García C, Grace LR. Long-term durability of a water-contaminated quartz-reinforced bismaleimide laminate. Polym Compos 2018;39(8):2643–9. https://doi.org/10.1002/pc.24255.

[19] Grace LR. Projecting long-term non-Fickian diffusion behavior in polymeric composites based on short-term data: a 5-year validation study. J Mater Sci 2016;51(2):845–53. https://doi.org/10.1007/s10853-015-9407-0.

[20] Grace LR, Altan MC. Three-dimensional anisotropic moisture absorption in quartz-reinforced bismaleimide laminates. Polym Eng Sci 2014;54(1):137–46. https://doi.org/10.1002/pen.23549.

[21] Grace LR, Altan MC. Non-fickian three-dimensional hindered moisture absorption in polymeric composites: Model development and validation. Polym Compos 2013;34(7):1144–57. https://doi.org/10.1002/pc.22523.

[22] Grace LR, Altan MC. Characterization of anisotropic moisture absorption in polymeric composites using hindered diffusion model. Compos Part A Appl Sci Manuf 2012;43(8):1187–96.

[23] Soles CL, Yee AF. A discussion of the molecular mechanisms of moisture transport in epoxy resins. J Polym Sci Part B Polym Phys 1999;38:707–15. https://doi.org/10.1002/(SICI)1099-0488(20000301)38.

[24] Guha RD, Idolor O, Grace L. An atomistic simulation study investigating the effect of varying network structure and polarity in a moisture contaminated epoxy network. Comput Mater Sci 2020;179:109683. https://doi.org/10.1016/j.commatsci.2020.109683.

[25] Vuković F, Walsh TR. Moisture ingress at the molecular scale in hygrothermal aging of fiber-epoxy interfaces. ACS Appl Mater Interfaces 2020;12(49):55278–89. https://doi.org/10.1021/acsami.0c1702710.1021/acsami.0c17027.s001.

[26] Bao L-R, Yee AF. Moisture diffusion and hygrothermal aging in bismaleimide matrix carbon fiber composites: Part II-woven and hybrid composites. Compos Sci Technol 2002;62(16):2111–9. https://doi.org/10.1016/S0266-3538(02)00162-8.

[27] Idolor O, Guha RD, Berkowitz K, Grace L. An experimental study of the dynamic molecular state of transient moisture in damaged polymer composites. Polym Compos 2021;42(7):3391–403. https://doi.org/10.1002/pc.26066.

[28] Takeshita Y, Becker E, Sakata S, Miwa T, Sawada T. States of water absorbed in water-borne urethane/epoxy coatings. Polym (United Kingdom) 2014;55(10):2505–13. https://doi.org/10.1016/j.polymer.2014.03.027.

[29] Jelinski LW, Dumais JJ, Cholli AL, Ellis TS, Karasz FE. Nature of the water-epoxy interaction. Interaction 1985;18(6):1091–5.

[30] Moy P, Karasz FE. Epoxy-water interactions. Polym Eng Sci 1980;20(4):315–9. https://doi.org/10.1002/pen.760200417.

[31] Grace LR. The effect of moisture contamination on the relative permittivity of polymeric composite radar-protecting structures at X-band. Compos Struct 2015;128:305–12. https://doi.org/10.1016/j.compstruct.2015.03.070.

[32] Musto P, Ragosta G, Mascia L. Vibrational spectroscopy evidence for the dual nature of water sorbed into epoxy resins. Chem Mater 2000;12(5):1331–41. https://doi.org/10.1021/cm9906809.

[33] Berkowitz K, Idolor O, Pankow M, Grace L. Combined effects of impact damage and moisture exposure on composite radome dielectric properties. Int. SAMPE Tech. Conf., vol. 2018- May, 2018.

[34] García C, Fittipaldi M, Grace LR. Epoxy/montmorillonite nanocomposites for improving aircraft radome longevity. J. Appl. Polym. Sci. 2015;132(43).

[35] Gilard V, Martino R, Malet-martino M, Riviere M, Gournay A, Navarro R. Measurement of total water and bound water contents in human stratum corneum by in vitro proton nuclear magnetic resonance spectroscopy. Int J Cosmet Sci 1998;20(2):117–25. https://doi.org/10.1046/j.1467-2494.1998.171743.x.

[36] Guan L, Xu H, Huang D. The investigation on states of water in different hydrophilic polymers by DSC and FTIR. J Polym Res 2011;18(4):681–9. https://doi.org/10.1007/s10965-010-9464-7.

[37] Abdelmola F, Carlsson LA. State of water in void-free and void-containing epoxy specimens. J Reinf Plast Compos 2019;38(12):556–66. https://doi.org/10.1177/0731684419833469.

[38] Guha RD, Idolor O, Berkowitz K, Pasquinelli M, Grace LR. Exploring secondary interactions and the role of temperature in moisture-contaminated polymer networks through molecular simulations. Soft Matter 2021;17(10):2942–56. https://doi.org/10.1039/D0SM02009E.

[39] Guha RD, Idolor O, Grace L. Molecular Dynamics (MD) simulation of a polymer composite matrix with varying degree of moisture: investigation of secondary bonding interactions. Am. Soc. Compos. 2019, Lancaster, PA: DEStech Publications, Inc.; 2019. https://doi.org/10.12783/asc34/31367.

[40] Krupka J. Precise measurements of the complex permittivity of dielectric materials at microwave frequencies. Mater Chem Phys 2003;79(2-3):195–8. https://doi.org/10.1016/S0254-0584(02)00257-2.

[41] El-Koka A, Cha KH, Kang DK. Regularization parameter tuning optimization approach in logistic regression. Int Conf Adv Commun Technol ICACT 2013:13–8.

[42] Bisong E. Google colaboratory. Build. Mach. Learn. Deep Learn. Model. Google Cloud Platf., Berkeley, CA: Apress; 2019, p. 59–64. https://doi.org/10.1007/978-1-4842-4470-8_7.

[43] Wan X. The influence of polynomial order in logistic regression on decision boundary. IOP Conf Ser Earth Environ Sci 2019;267(4):042077. https://doi.org/10.1088/1755-1315/267/4/042077.

[44] Duchene P, Chaki S, Ayadi A, Krawczak P. A review of non-destructive techniques used for mechanical damage assessment in polymer composites. J Mater Sci 2018;53(11):7915–38. https://doi.org/10.1007/s10853-018-2045-6.

[45] Krupka J, Gregory AP, Rochard OC, Clarke RN, Riddle B, Baker-Jarvis J. Uncertainty of complex permittivity measurements by split-post dielectric resonator technique. J Eur Ceram Soc 2001;21(15):2673–6. https://doi.org/10.1016/S0955-2219(01)00343-0.

[46] Krupka J. Frequency domain complex permittivity measurements at microwave frequencies. Meas Sci Technol 2006;17(6):R55–70. https://doi.org/10.1088/0957-0233/17/6/R01.